AGGLOMERATES WITHIN BALL-MILLED LIGNOCELLULOSIC PARTICLES USING MINIMUM CRYSTAL SIZES

[1*] **Bello S. A.**

[1]Department of Materials Science and Engineering, Kwara State University, Malete, Nigeria
*Corresponding author's email address: sefiu.bello@kwasu.edu.ng or
adekunleshaafiu@gmail.com; 08038548418

ABSTRACT

The drive to reduce weight of transport and construction materials has drawn attention of researchers globally towards development of light weight composites. Particle agglomerates create region of discontinuity or weak particle adhesion to the matrix and impair mechanical properties of composites. In nanoparticles synthesis using ball-milling technique, formation of agglomerates can be controlled through milling parameters optimisation. In this study, coconut shell (lignocellulosic) nanoparticles have been synthesised by varying the charge ratios from 2.5 to 40 at constant milling duration (70 hours), speed of drum/vial rotation (194 revolution per minute) and ball sizes (5- 60 mm). Epoxy/coconut shell particulate composites were developed and characterized. Results indicated a reduction in particle sizes below 10 CRs. 100 and 41% increases in tensile strength and impact energy with 8.16 % reduction in tensile elongation was observed at 12 wt% of coconut shell nanoparticle addition. Hence coconut shell nanoparticles are confirmed for reinforcing epoxy for composite productions.

KEYWORDS: *Coconut shell; Mechanical Properties; X-ray study; Agglomerates; Epoxy*

INTRODUCTION

The drive to reduce weight of transport and construction materials has drawn attention of researchers globally towards development of light weight composites (Bello *et al.*, 2015b; America's Plastic Maker, 2016). Both synthetic and natural fibres are potential materials for matrix reinforcement (Deng *et al.*, 2007; Bhandakkar *et al.*, 2014; Padmavathi and Ramakrishnan, 2014; Rahman and Rashed, 2014; Agunsoye *et al.*, 2015; Alaneme and Sanusi, 2015; Bello *et al.*, 2015d; Agunsoye *et al.*, 2016b; Alaneme *et al.*, 2016). Synthetic fibres are highly expensive and contributing to high cost of composite production which prevents their widespread applications in engineering structures (The United Kingdom composites Industry, 2013). Agricultural products release huge amount of wastes such as coconut coir (Bello *et al.*, 2106), coconut shell (Bello *et al.*, 2015a; Bello *et al.*, 2015c), delonix regia seed (Agunsoye *et al.*, 2017), ground nut shell (Alaneme *et al.*, 2016), bagasse ash (Aigbodion, 2014), breadfruit seed hull (Atuanya *et al.*, 2012), egg shell (Agunsoye *et al.*, 2015; Hassan and Aigbodion, 2015), animal bone (Asuke *et al.*, 2012; Asuke *et al.*, 2014) and bean pods (Atuanya *et al.*, 2014) which are renewable sources of natural fibres for composite

developments. Moreover, recycling of wastes from both agricultural produce and industry support environmental cleanliness, green economy which is based on energy efficiency and reduction in green gas emission (Hunton, 2005; Kamberović *et al.*, 2009; Manufacturer, 2012).

Practices over years are processing of agricultural wastes to micro-sized particles but exceptional properties of nanoparticles have gained attention of many researchers, giving rise to dispersion strengthening composites or nanocomposites. Nanoparticles can be engineered or non-engineered for a purpose or produced due to natural occurrences. Synthesis of nanoparticles is usually followed with informative property analyses to determine their sizes, examine their morphology and other necessary properties (Pokropivny *et al.*, 2007). In determination of nanoparticle sizes, different approaches including theoretical calculation and image sizing have been reported (Wang, 2000; Wang, 2003; Bello *et al.*, 2018b).

Recent interest on using agricultural waste particles for reinforcing polymer to produce dispersion strengthening composites for engineering applications has paved way for researches into particle synthesis using different techniques (Bello *et al.*, 2015b; Bello, 2017). Agricultural waste particle production by ball-milling, a type of top-down approach has been reported (Essl *et al.*, 1999; Sommer *et al.*, 2006; Breitung-Faes and Kwade, 2008; Knieke *et al.*, 2010; Sarki *et al.*, 2011; Prasad Yadav *et al.*, 2012). Although, synthesis of agricultural waste nanoparticles is found, particle agglomeration is a challenge (Sommer *et al.*, 2006; Bello *et al.*, 2015a).

Particle agglomeration is an integration/fusion of ultrafine particles during synthesis. It occurs when particles attain unstable high energy state because of their minimum sizes. However, ultrafine particles seek energy minimization through fusion with one another and or with coarse particles to improve their stability. Consequently, formation of particle colonies known as agglomerates occur. Particle agglomeration results in relative particle coarsening and opposes the particle refinement which is the purpose of ball-milling. On the other hand, presence of agglomerates forming parts of synthesised agricultural waste particles create region of discontinuity within a matrix when such particles are for reinforcing matrix for composite development.

Furthermore, impairment of mechanical properties of the composites due to particle agglomerates have been revealed in literatures (Agunsoye and Aigbodion,

2013; Atuanya *et al.*, 2014). Therefore, this justifies optimisation of ball milling parameters such as charge ratios, milling duration, vial speed of rotation, size and nature of the milling balls for producing agricultural waste particles with little or no particle agglomerates. Effects of milling durations and vacuum carbonisation on properties of coconut shell nanoparticles with mathematical optimization of charge rations have been studied and reported earlier by (Bello *et al.*, 2015a; Bello *et al.*, 2015c; Bello *et al.*, 2018b; Bello *et al.*, 2106). However, this study discloses influence of charge ratios on sizes and morphologies of coconut shell particles and mechanical properties of epoxy nanocomposites developed using the synthesized uncarbonized coconut shell nanoparticles.

MATERIALS AND METHODS

Uncarbonized coconut shell nanoparticles (UCSnp) used in this work were synthesised by ball milling technique using 37 μm sized coconut shell powders as a precursor in accordance with (Bello *et al.*, 2015a; Bello *et al.*, 2015c). Precursors were milled at varying CRs, ranging from 2.5 to 40 while other milling parameters such as milling duration (70 hours), speed (194 rpm) and sizes/ materials of the milling balls were kept constant. UCSnp were analysed using Scanning Electron Microscope/Energy Dispersive X-ray spectroscopy (ASPEX 3020, SEM/EDX), Transmission Electron Microscope (Philip 301) and X-ray diffractometer (XRD). Epoxy composites were developed using precursor coconut shell powders (UCSmp) and UCSnp obtained by milling for 70 hours at 10 CRs. The method of production of the composite is in line with (Bello *et al.*, 2019) with little modification. Structural and mechanical properties of the epoxy/uncarbonized coconut shell nanoparticles (E/UCSnp) were examined.

RESULTS AND DISCUSSION

Microstructures of Uncarbonised Coconut Shell Nanoparticles

Fig. 1 shows the SEM/EDX of the bulk coconut shell which is the source of the precursor. Micrograph in Fig. 1 reveals the coconut shell as a solid body with surface discontinuities. The defects make the coconut shell to appear as having many individual layers joining together to assume a singular geometric body. Energy dispersive X-Ray chemical analysis shows that the bulk coconut shell contains C, O, Na, Al, Si, P and K. This agrees with (Bello *et al.*, 2015a; Bello *et al.*, 2015c; Bello *et al.*, 2018b).
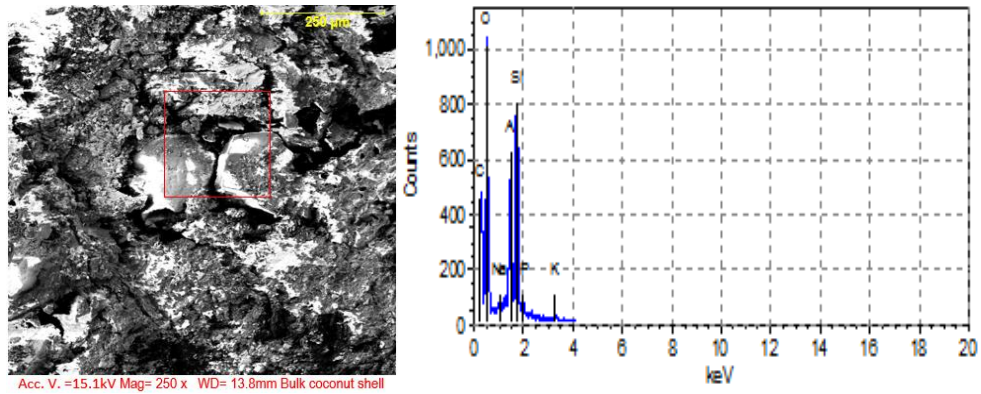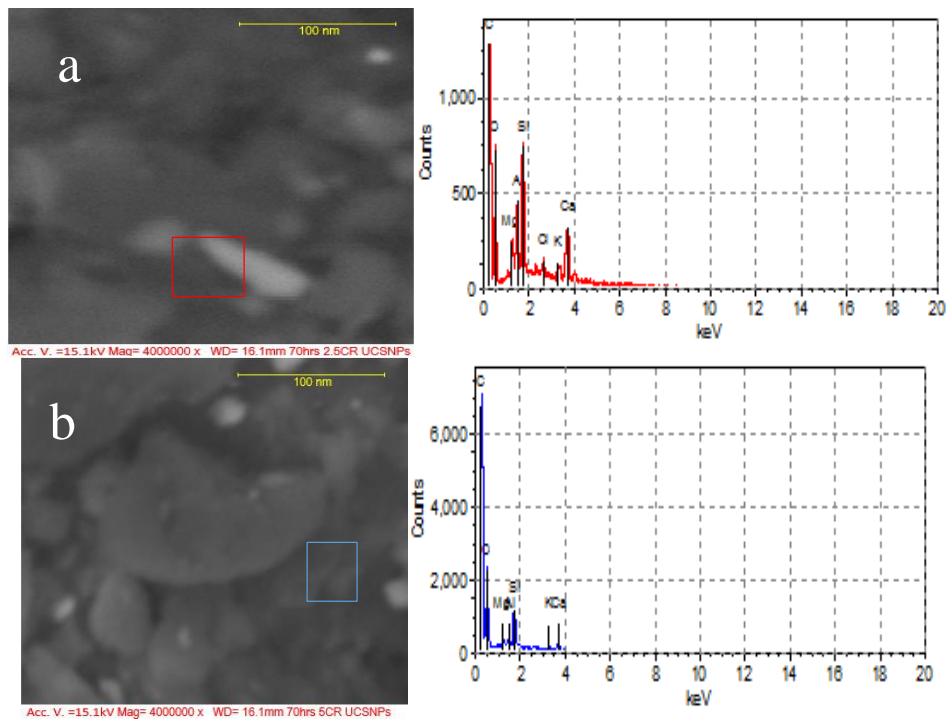
Fig. 1. SEM/EDX of sourced bulk coconut shell

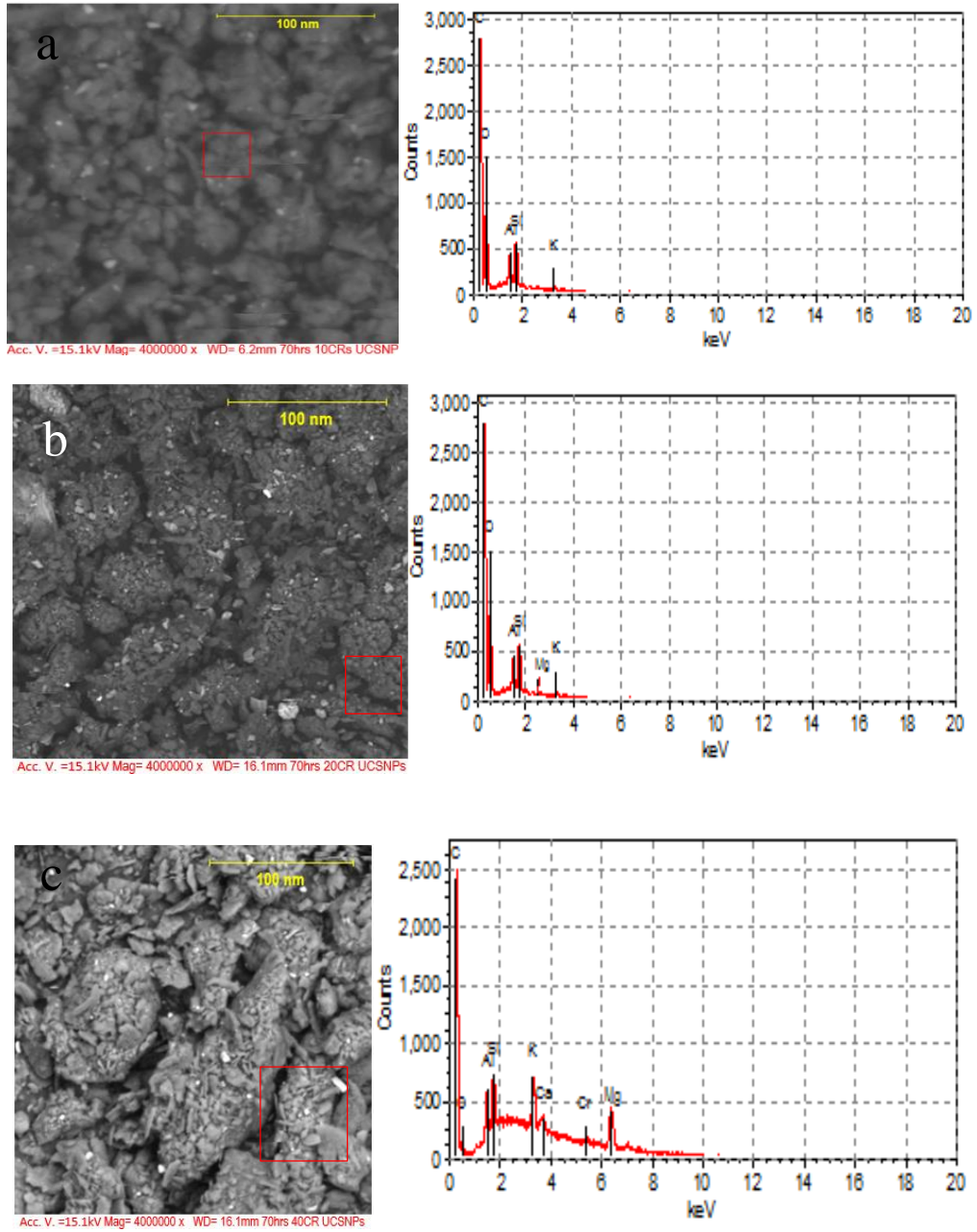**Fig. 2. SEM/EDX of UCSnp at (a) 2.5 CRs, (b) 5 CRs (Bello *et al.*, 2018b)**

Fig. 3. SEM/EDX micrographs of UCSnp at a) 10 CRs (26), b) 20 CRs c) 40 CRs

Coconut shell being organic material is expected to be rich in carbons. However, maximum peak belonging to O rather than C can be linked with the wetness of the bulk coconut shells while on the other hands, presence of inorganic compounds due to Na, Al, Si, P and K in the coconut shells may also contribute to maximum peak observed with O. SEM in Fig. 2(a-b) reveals the morphology of the UCSnp obtained at 2.5 and 5 CRs and constant milling duration of 70 hours. UCSnp appears dull having different sizes and shapes with an individual UCSnp can easily be distinguished from one another. This was an indication that there was a gradual breakage of the precursor powders during the milling process with no sign of particle agglomeration. Uncarbonized coconut shell nanoparticles in Fig. 2(b) appear smaller and less dull than their counterparts in Fig. 2(a). Elemental compositions of UCSnp in Fig. 2 agree with that of bulk coconut shell in Fig. 1. However, in terms of peak height, C has a greater peak than O. C peak in Fig. 2(a) has a height of about 1300 counts, 73 % higher than that of O peak while in Fig. 2(b), C peak is 250 % taller than that of O. Rise in the C peak and fall in O peak could be associated with dryness of the UCSnp due to temperature induced friction occurred, during the course of ball milling. SEM micrograph in Fig. 3 shows the morphologies of UCSnp obtained at 10, 20 and 40 CRs. It is observed from Fig. 3 that UCSnp exist in form of fused solid bodies with different shapes, sizes and varied degree of particle integration or agglomeration. The degree of particle integration increased as shown in Fig. 3 as the CR rose from 10 to 40. However, agglomerated particles in Fig. 3(b-c) show many fine particles which has been fused together due to increased surface area to volume ratio as the particle reduction was in progress during the course of ball milling. During the milling process, rotation of the mill vial caused continual jumping of grinding balls and particles during which the coconut shell particles collided with the milling balls and inner wall of the vial.
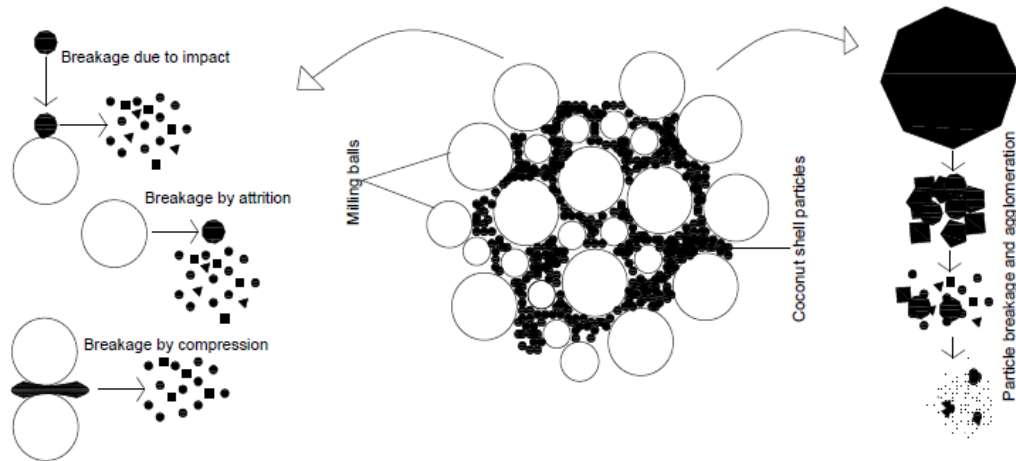
Fig. 4. Computer image showing particle breakage and agglomeration during the milling process

This resulted in dissociation of the particles at point of tangential collisions between two balls or a ball and the inner surface of the drum/vial. Extent of breakage increased as the CRs increased from 2.5 to 40 CRs due to greater kinetic energy with which the balls stroke the particles. Comparison of Fig. 2 with Fig. 3 demonstrated that there was a gradual breakage of the precursor particle, leading to formation of fine particles from the coarse particles. As the breakage continued, surface area of the newly formed fine particles increased. The increment in the surface energy make the particle thermodynamically unstable especially above 10 CRs. This caused the fusion or integration of fine particles (see Fig. 4) in order to seek minimum energy state of natural comfort, serving as a driving force for the formation of agglomerated particles as shown in Fig. 3(b-c).

TEM Images of Uncarbonised Coconut Shell Nanoparticles
Figure 5 presents the TEM images of the UCSnp obtained at different CRs. The TEM images reveal each particle individually in approximately spherical shape with different degrees of particle agglomeration. By comparing the images from Fig. 5(a-e), it was observed that UCSnp appear smaller as the CRs increased until above 10 CRs when the particle seemed bigger than their counterparts from 10 CRs and above. The bigness of the UCSnp above 10 CRs could be ascribed to their fineness which enhanced their surface area, leading to particle interfacial adhesion.
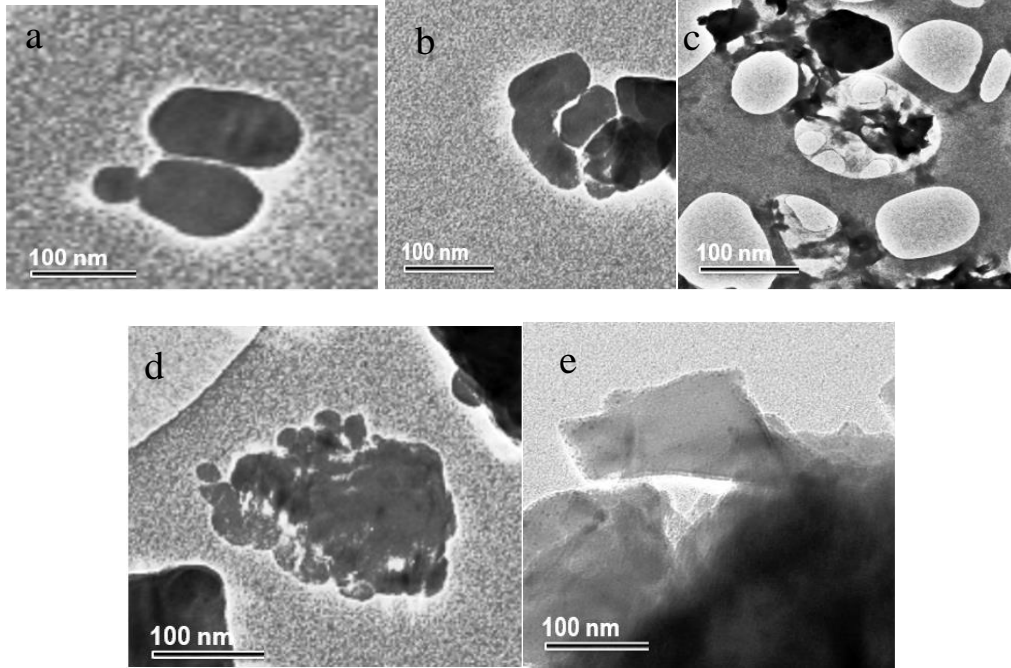
Fig. 5. TEM images of UCSnp obtained at a) 2.5 CRs, b) 5 CRs (30), c) 10 CRs, d) 20 CRs e) 40 CRs

The ball impacts on the particles caused breakages of the particle at every collision between balls and UCSnp. This enhanced the Vander Waal's attraction and other intermolecular energy among the particles, leading to their fusion or clustering. Similar observation was made with the SEM micrographs in Fig. 3.

X-Ray Diffraction of Uncarbonised Coconut Shell Nanoparticles
Figures 6-10 show the XRD profiles of UCSnp obtained at different CRs. Diffractogram in Fig. 6 revealing XRD profile of UCSnp obtained at 2.5 CRs, depicts phases such as C; $Al_2Si_2O_5(OH)_4$ and SiO_2 at different diffraction angles (2θ) ranging from 0 to $80°$. The same phases are observed in the XRD profiles of UCSnp obtained at 5 CRs in Fig. 7 while the phases of UCSnp obtained at 10 CRs in Fig. 8 are SiO_2 and C_2CaMgO_6 (Bello *et al.*, 2015a).
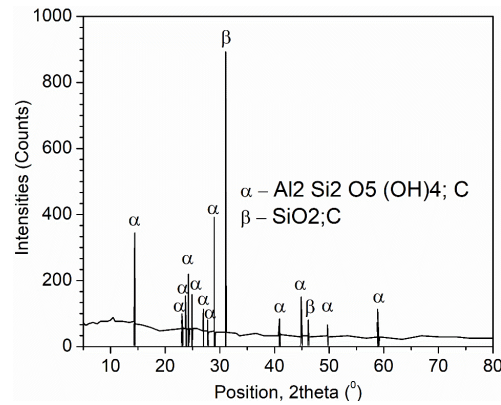
Figure 6: XRD profiles of uncarbonised coconut shell nanoparticles obtained at 2.5 charge ratios

Consistency of C and SiO_2 in Fig. 6-9 is an indication that coconut shell is very rich in carbon which exists in different forms of organic compounds such as cellulose and lignin while Si exists in inorganic forms. Formation of compounds such as $Al_2Si_2O_5(OH)_4$ and C_2CaMgO_6 and C as an individual compound/element can be linked to chemical interaction of various constituents of coconut shell particles during the milling process (Bello *et al.*, 2018b). Figures 9-10 depict the XRD profiles of UCSnp obtained at 20 and 40 CRs. It is observed that C and SiO_2 are the only phases present. Absence of $Al_2Si_2O_5(OH)_4$ and C_2CaMgO_6 can be linked to agglomerated particles of C and SiO_2 which might have blocked the reflected X-Ray from $Al_2Si_2O_5(OH)_4$ and C_2CaMgO_6 during the XRD analysis. Similar observation was made by (Liu *et al.*, 2013). By comparing the XRD profiles in Fig. 6-10; it is observed that the count score corresponding to the maximum peak of each diffractometry increases with an increment in the CRs.
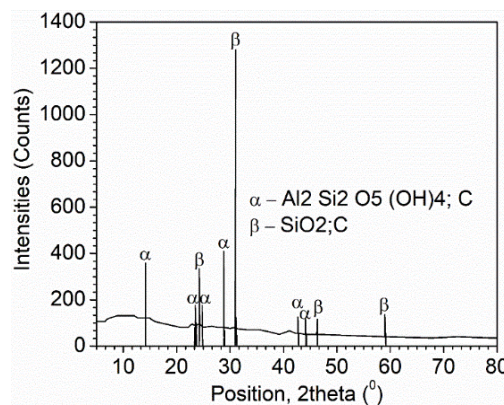
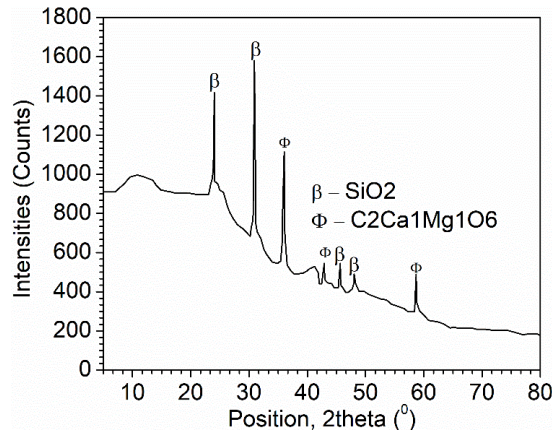**Figure 7: XRD profiles of uncarbonised coconut shell nanoparticles obtained at 5 CRs charge ratios**

Fig. 8. XRD profiles of uncarbonised coconut shell nanoparticles obtained at 10 charge ratios
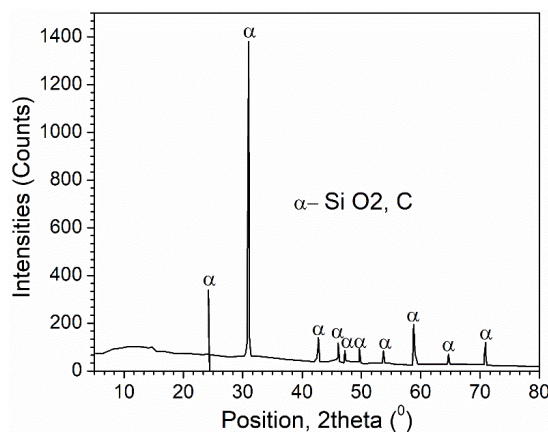

Fig. 9. XRD profiles of uncarbonised coconut shell nanoparticles obtained at 20 charge ratios

Also, an increment in the peak widths reflects the increased peak broadness as the CRs increases up to 10 (see Fig. 6-8). Above 10 CRs, further peak broadness is not noticeable (see Fig. 9-10). The peak broadness up to 10 CRs indicated a continual breakage of coconut shell particles resulting in a decrease in their sizes. However, above 10 CRs, fine particles having high surface energy adhered with one another to form bigger particles with reduced surface energy. In the previous work, similar agglomeration was observed with uncarbonised and carbonised coconut shell nanoparticles above 46 and 16 hours of milling respectively at 10 CRs (Bello *et al.*, 2015a; Hassan *et al.*, 2015; Bello *et al.*, 2106). Since the UCSnp

and CCSnp are synthesised to serve as nanoparticles for polymeric composite fabrication (Bello *et al.*, 2015b; Agunsoye *et al.*, 2016a), optimisation of ball milling parameters are important to obtain nanoparticle with little or no agglomeration. Agglomeration of nanoparticle is undesirable in a matrix for composite development. This acts as a region of discontinuity within the matrix and reduce mechanical properties of the composites (Asuke *et al.*, 2012).
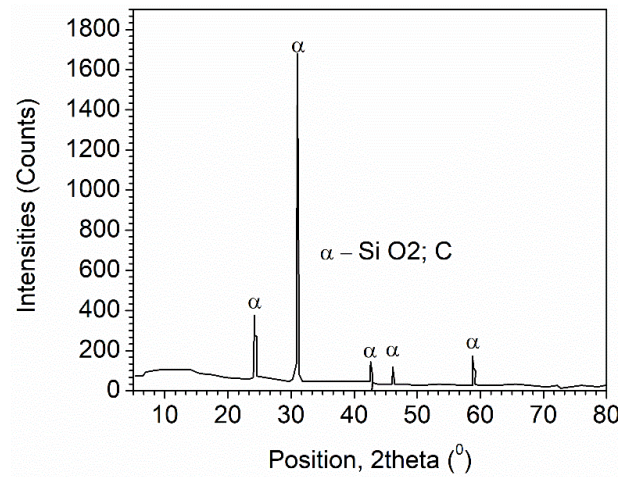

Fig. 10. XRD profiles of uncarbonised coconut shell nanoparticles obtained at 40 charge ratios

Sizes of Coconut Nanoparticles

Sizes of UCSnp were determined from TEM (see Fig. 5) supported with Gwyddion software. UCSnp obtained at 2.5 CRs and 70 hours has the approximate size between 4 and 200 nm. Size of UCSnp at 5 CRs and 70 hours varying from 4 to 149 nm. Sizes of UCSnp at 10 CRs and 70 hours varies between 0 and 136 nm, respectively. Sizes of UCSnp at 20 CRs are between 0 and 101 nm while minimum and maximum sizes of UCSnp at 40 CR are 1.1 and 107.4 nm, respectively (see Fig. 5). Minimum sizes of UCSnp obtained from XRD at 2.5, 5, 10, 20 and 40 CRs are 11.8, 10.95, 2.95, 7.97 and 13.43 nm, respectively. The respective maximum sizes are 133.07, 113.11, 153.58, 97.28 and 266.43 nm (Bello *et al.*, 2018b). Average sizes of UCSnp obtained from TEM, SEM and XRD were matched as shown in Fig. 11. Generally, observation from Fig. 11 was that the average sizes decreased with an increment in CRs. The decrease in the average sizes is very noticeable up to 10 CRs. Above 10 CRs, further reduction in the average particle size is unnoticeable as indicated by SEM and XRD while TEM reveals a gradual decrease in the sizes though the decrease is not as high as

what is observed below 10 CRs. Therefore, this justifies the reason for using UCSnp obtained at 10 CRs and 70 hours of milling for the epoxy/uncarbonised coconut shell nanoparticle (E/UCSnp) development.

Possible proposition to the above observation is the balance between further reduction in particle size and particle agglomeration above 10 CRs. As the milling progressed, uneven distribution of the ball impacts on the particles caused differences in the particle breakages. This resulted in the presence of fine and relatively coarse particles at any instance of the ball milling. An increase in CRs enhanced the magnitudes of the ball impacts on the particle with consequent particle refinement and agglomeration. Balance between particle refinement and agglomeration is justified by the attainment of minimum sizes by lignocellulosic particles. At minimum sizes, UCSnp are characterised with high surface energy. That is, they are thermodynamically unstable. Agglomeration of fine particles minimise their energy and restore their stability.
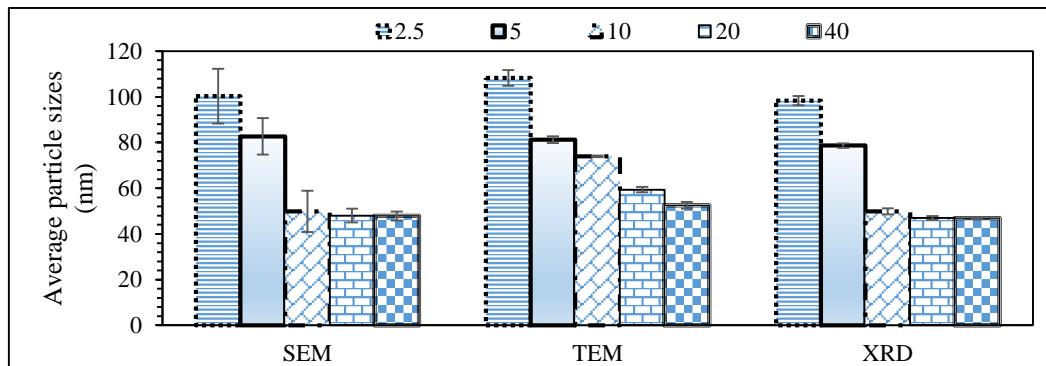

Figure 11: Average sizes of uncarbonised coconut shell nanoparticles

Structural Properties and Mechanical Properties of Epoxy Coconut Shell Nanocomposites

Figures 12-15 depict XRD profiles of epoxy/coconut shell composites containing 2 wt% UCSmp, 10wt% UCSmp, 2wt% UCSnp and 10wt% UCSnp, respectively. Detected phases are both organic and inorganics which are ceramics in nature (see Tables 1-4). Presence of the phases are evidence of chemical reaction among epoxy resin, hardener and coconut shell particulate reinforcement. Being ceramics in natures, their ions and or molecules are bonded together by ionic, covalent and or dative bonding. Therefore, they possess octet configuration which enable their stabilities and are expected to be hard, rigid and resistant to chemical attacks. As second phase compounds within the epoxy, they interact with the composite

mobility under loading resulting in an improvement in the load bearing capacity of the epoxy matrix.

Table 1: Identification of phases occupying the matrix of epoxy/2UCSmp composite

Pos. [°2Th.]	Height [cts]	Compound Name	d-spacing [Å]	Chemical Formula
18.77	6359	Magnesium Nitrate Hydrate	4.7	$MgN_2O_3.4H_2O$
19.55	6338	Hydrogrossular	4.5	$Ca_3Al_2O_6(H_2O)_6$
18.44	6332	Magnesium Oxide Carbonate	4.3	$Mg_3O(CO_3)_2$
18.76	6359	Diphenylmethlamine	4.7	$(C_6H_5)_2NCH_3$
18.76	6359	Urea	4.7	$CO(NH_2)_2$

Table 2: Identification of phases within the matrix of epoxy/10UCSmp composite

Pos. [°2Th.]	Compound Name	d-spacing [Å]	Chemical Formula
42.64	Cliftonite	2.1	C
18.50	Nordstrandite	4.5	$Al(OH)_3$
42.64	Periclase	2.1	MgO
42.64	Magnesium Oxide Carbonate	2.12	$Mg_3O(CO_3)_2$
30.85	Ammonium Chlorate	2.9	NH_4ClO_4
20.87	Calcium Nitrite Hydrate	4.26	$Ca(NO2)_2.4 H_2O$
18.50	Aluminium Acetate Hydroxide	4.50	$C_4H_7AlO_5$
18.50	Aluminium Formate	4.5	$C_3H_3AlO_6$
42.64	Fullerite	2.1	C_{60}
42.64	Carbon Nitride	2.1	C_3N_4

Table 3: Identification of second phase particles within epoxy/2UCSnp composite

Pos. [°2Th.]	Compound Name	d-spacing [Å]	Chemical Formula
22.06	Urea	4.0	CH_4N_2O
40.32	Calcium Amide	2.2	$Ca(NH_2)_2$
17.49	Calcium Nitrite Hydrate	5.1	$Ca(NO_2)2.4H_2O$
36.76	Aluminium Chloride Hydroxide Hydrate	2.44	$AlC_{l3}.2Al(OH)_3.6H_2O$
36.76	Gibbsite, syn	2.44	$Al(OH)_3$
34.82	Fullerite	0.000	C60
34.82	Earlandite, syn	2.57	$Ca_3(C_6H_5O_7)_2.4H_2O$
36.76	Caldecahydrite [NR]	2.4	$CaAl_2O_4.10H_2O$
79.40	Calcium Tetraoxide	1.2	CaO_4
80.57	Aluminium Chloride Graphite	1.2	$AlCl_3C_x$

Table 4: Identification of second phase particles within epoxy/10UCSnp composite

Pos. [°2Th.]	Compound Name	d-spacing [Å]	Chemical Formula
18.11	Magnesium Oxalate Hydrate	4.9	$C_2MgO_4.H_2O$
20.26	Ammonium Chlorate	4.4	NH_4ClO_4
42.59	Magnesium Oxide Carbonate	2.1	$Mg_3O(CO_3)_2$
19.72	Potassium benzene oxide	4.7	$K_3C_6H_5O$
68.42	Ammonium Chloride	1.4	NH_4Cl
49.20	Magnesium Chlorate Hydrate	1.9	$Mg(ClO_4)_2.3H_2O$
20.26	Magnesium Chlorate Urea	4.4	$C_6H_{24}N_{12}O_6Mg(ClO_3)_2$
84.52	Calcium Hydroxide	1.1	$Ca(OH)_2$
87.36	Magnesium Chlorate	1.1	$Mg(ClO_4)_2$

Figure 12:X-ray profiles of epoxy/2UCSmp composite

Figure 13:X-ray profiles of epoxy/10UCSmp composite

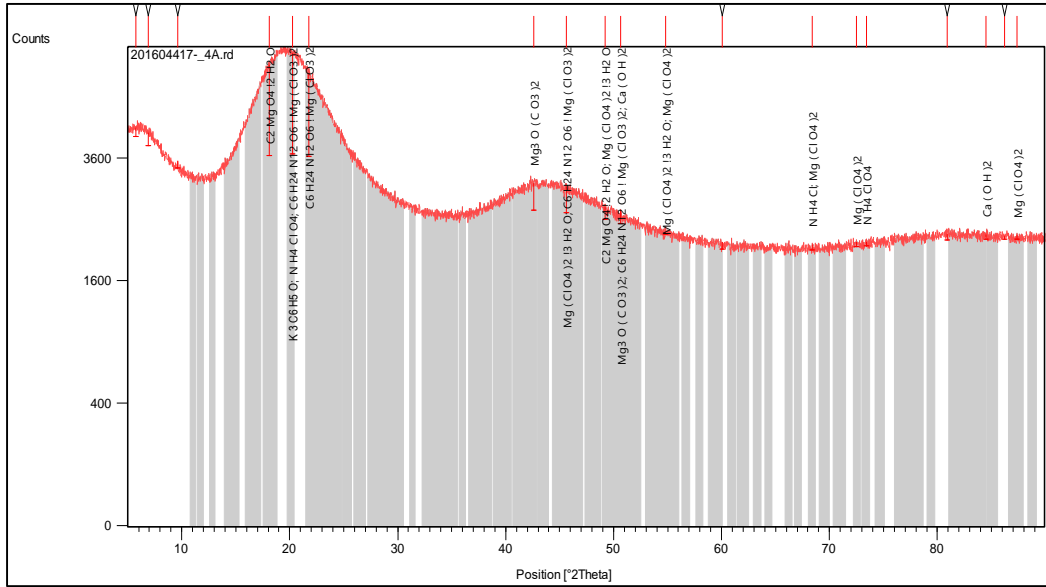**Figure 14: XRD profile of epoxy/2UCSnp composites**

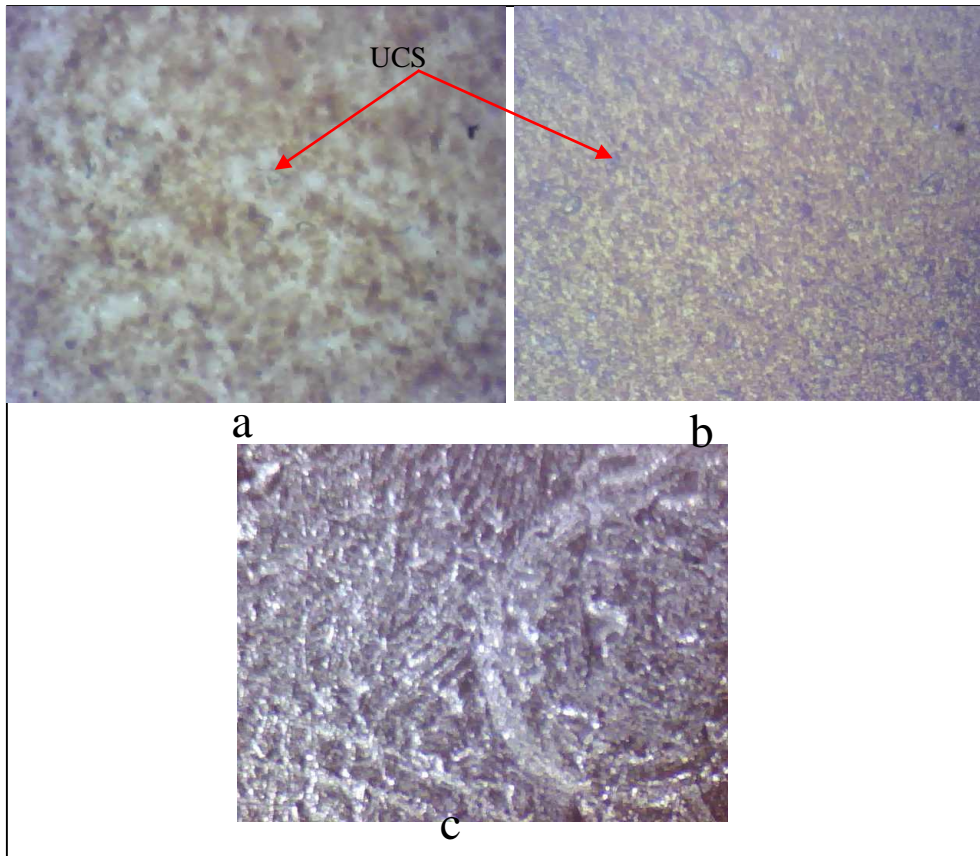**Figure 15: XRD profiles of epoxy/10UCSnp composite**

Figure 16: Optical micrographs (a) epoxy/2UCSnp (b) epoxy/6UCSnp (c) epoxy/10UCSnp (X 100)

It is observed that different phases belong to the composites with fineness and an increase in wt% of the coconut shell particles. Evidence for this is the detection of C, C_{60} and C_3N_4 in E/10% UCSmp (See Table 2) which are absent in E/2% UCSmp containing smaller wt%. With fineness of the coconut shell particles, CaO_4; $AlCl_3C_x$ (See Table 3); $Mg(ClO_4)_2$ and $C_6H_{24}N_{12}O_6Mg(ClO_3)_2$ (see Table 4) were confirmed in addition to existing phases within the epoxy microparticle composites. This observation can be linked with increasing number of particles and surface area with an increase in wt% and fineness of the coconut shell particles, respectively. It is an established fact that rate of chemical reaction increases with concentration and the area exposed (Janik *et al.*, 2014). Therefore, the additional phases within the epoxy have tendency to create more straining effect with an increase in mechanical performance of the composites. Microstructures in Fig. 16 display second phase ceramic particles dispersed

homogeneously throughout the matrix without any form of particle agglomeration. Besides the even dispersion of the particles, they are strongly bonded to the matrix. This structural integrity is proportional to good mechanical performance of epoxy/UCSnp composites in terms of optimum combination of strength and ductility. SEM morphologies of epoxy/UCSnp composites in Fig. 17-19 affirm the microstructural integrity of the composites observed in the optical micrographs in Fig. 16. However, higher packing densities of the microstructures are related to wt% of UCSnp additions to epoxy matrix. Energy dispersive X-ray spectrographs indicate majorly presence of C and O which confirm the phases detected from the XRD study.
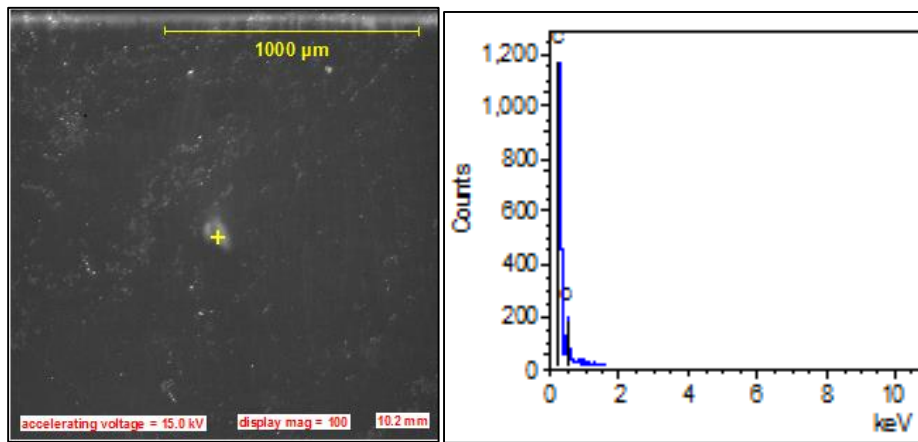

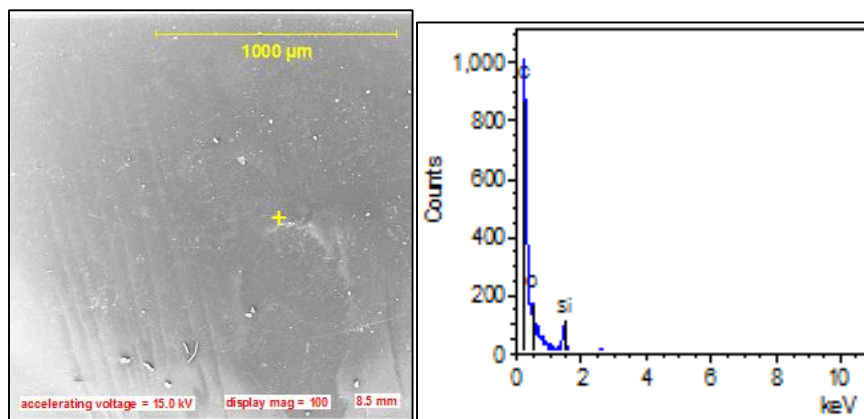**Figure 17: SEM/EDX of epoxy/2UCSnp composite**

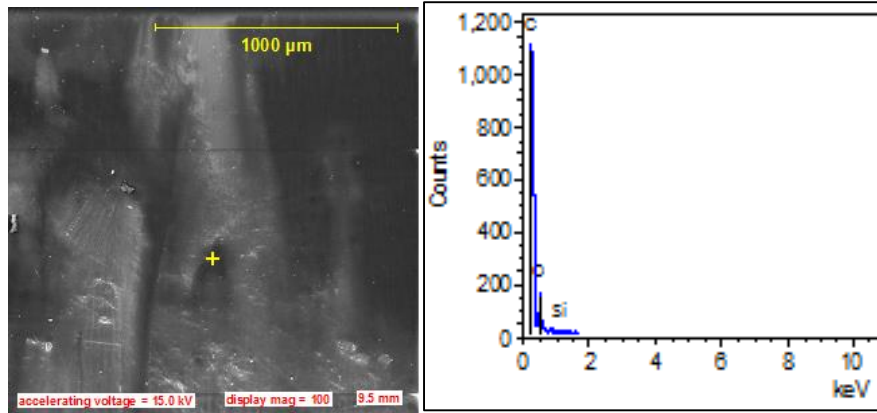**Figure 18: SEM/EDX of epoxy/6UCSnp composite**

Figure 19: SEM/EDX of epoxy/10UCSnp composite

Addition of coconut shell particles to the epoxy matrix yields an improvement in mechanical properties of the composites. It is observed from Fig. 20a that tensile strength values increase from 13.48 Nmm^{-2} of unreinforced epoxy to 24.18 and 26.97 Nmm^{-2} at 10wt% additions of uncarbonised coconut shell microparticles and nanoparticles. There is a prevailing increment in the tensile strength of epoxy/UCSmp and epoxy/UCSnp composites throughout the level of UCSmp and UCSnp reinforcements, implying that there is no sign of matrix saturation. Similar observation in respect of epoxy/UCSmp has been made in literature (Sarki *et al.*, 2011). The increase in the tensile strength of both epoxy/UCSmp and epoxy/UCSnp composites is linked with hard crystalline ceramic phases and the strong interfacial bonding between the phases and the epoxy matrix. Higher tensile strength developed by epoxy/UCSnp is related to better structural integrity observed with epoxy/UCSnp composites. However, the tensile elongations of epoxy/UCSnp composites are lower than those of epoxy/UCSmp composites. The conventional strength increment-elongation reduction is obeyed by both composites. An increase in impact energy of epoxy/uncarbonised coconut shell particulate composites with UCSmp and UCSnp particles additions is observed in Fig. 21. Epoxy/UCSnp nanocomposites display a higher impact energy (from 8.84 at 0 wt% to 12.43 J at 12 wt% UCSnp additions) at all levels of reinforcements than those (from 8.84 at 0 wt% to 10.01 J at 12 wt% UCSmp additions) of their microparticle composite counterparts. Generally, the increase in impact energy can be attached to presence of second phase particles which toughen the epoxy matrix. Higher impact energy of epoxy/UCSnp composites is related to higher packing density of the particles resulting from the fineness of the UCSnp featuring

within the matrix of epoxy/UCSnp. This offered higher resistance to sudden impact stress, thereby increasing energy absorption capacity of the composite.
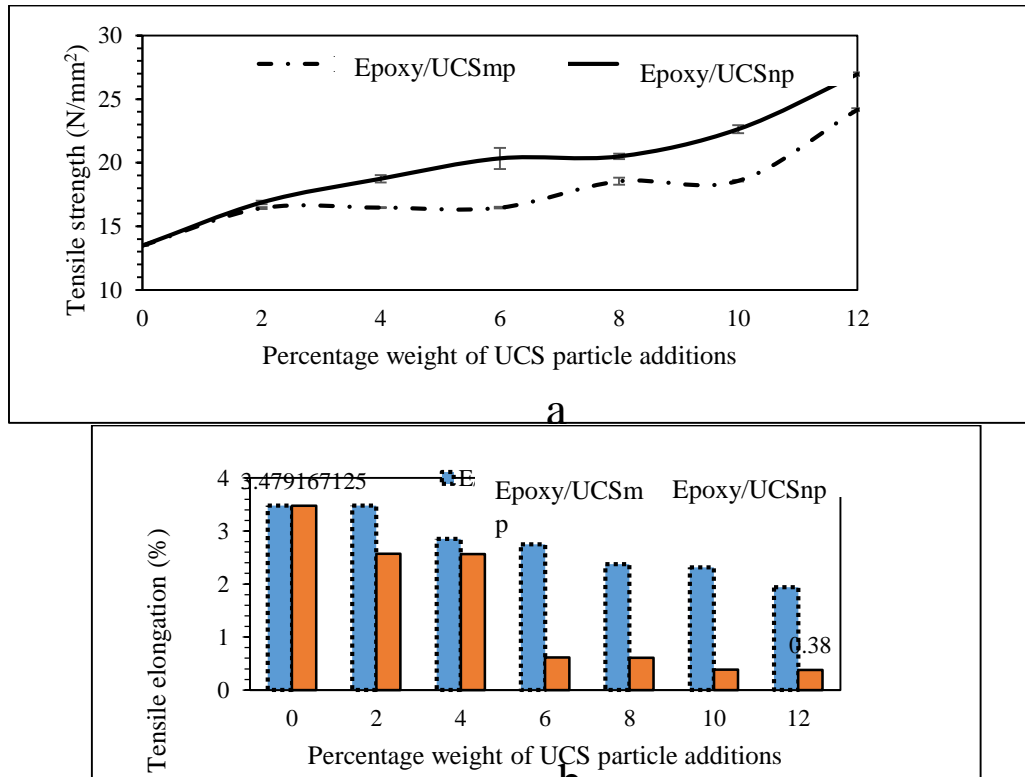

Figure 20: Tensile (a) strength (b) elongation of epoxy/UCSmp and epoxy/UCSnp composites
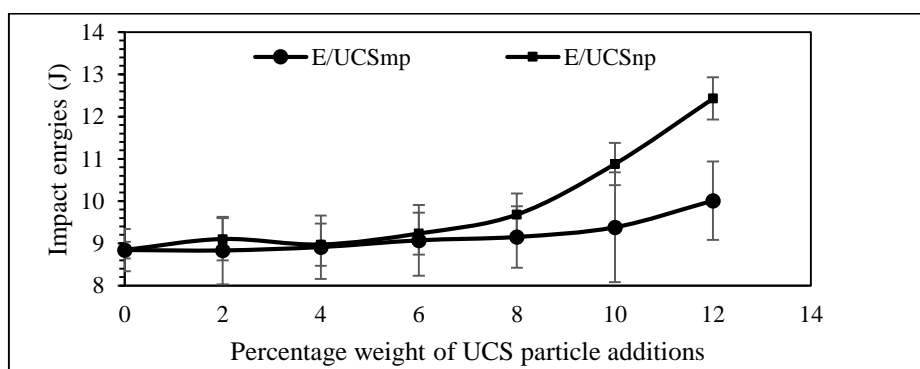

Figure 21: Comparison of impact energy of epoxy/UCSmp and epoxy/UCSnp composites

The difference in inter-planar spacing as observed in Tables 1-4 is an affirmation of the increased packing density of the particles embedded in the epoxy/UCSnp. Reports from literature have revealed improvement in epoxy composite due to carbonized coconut shell, aluminium (Bello *et al.*, 2017; Bello *et al.*, 2018b), copper (Pargi *et al.*, 2015), carbon nanotube (Zhang *et al.*, 2012; Wang *et al.*, 2016), E-Glass/jute (Deshpande and Rangaswamy, 2014) and coconut coir fibres (Natarajan and Balasubramanya, 2013; Akindapo *et al.*, 2014) which are in line with findings from this study. Similarly, possible use of epoxy/aluminium (Bello *et al.*, 2017; Bello *et al.*, 2018b), epoxy/ carbonized coconut shell and epoxy hybrid kenaf fibres (Davoodi *et al.*, 2010) for automobile bumper based on the comparison of properties of each composite with band standards (MatWeb Material Property Data, 2010) has been reported. A tensile strength of 26.97 Nmm^{-2} of the epoxy nanocomposite in this study greater than that of epoxy/aluminium composite (Bello *et al.*, 2018a) and impact energy, 12.43 J falls between 10-18 J as reported in (MatWeb Material Property Data, 2010; Bello *et al.*, 2018a) affirms suitability of the epoxy nanocomposite containing 12wt% nanoparticle reinforcement in this study for automobile bumper provided that its other properties such as flexural properties meet the band standards (MatWeb Material Property Data, 2010) for the bumper application.

CONCLUSIONS
Based on the experimental investigations carried out in this study, the following inferences were made:
1. Average coconut shell particle size at 10 charge ratios was the minimum.
2. Opposition of particle agglomeration to the particle refinement was apparent above at 10 charge ratios causing insignificant further reduction in the average sizes of uncarbonized coconut shell nanoparticles.
3. Addition of coconut shell nanoparticles to epoxy led to an increase in tensile strength and impact energy with slight reduction in percentage elongation.
4. A maximum tensile strength and impact energy of 26.97 Nmm^{-2} and 12.43 J, respectively were obtained at 12 wt% of the uncarbonized coconut shell nanoparticle addition to the epoxy against 13.47 and 8.88J of the pristine epoxy.
5. Uncarbonized coconut shell nanoparticle addition to the epoxy caused a higher improvement in mechanical properties of the epoxy composites than those of uncarbonized coconut shell microparticle addition.
6. Epoxy uncarbonized coconut shell composites may be a suitable material for automobile applications.

ACKNOWLEDGEMENT

REFERENCES

Agunsoye, J. O. and Aigbodion, V. S. (2013). Bagasse Filled Recycled Polyethylene Bio-composites: Morphological and Mechanical Properties Study. *Results in Physics, 3*, 187-194. doi: http://dx.doi.org/10.1016/j.rinp.2013.09.003.

Agunsoye, J. O., Bello, S. A. and Adetola, L. O. (2017). Experimental Investigation and Theoretical Prediction on Tensile Properties of Particulate Reinforced Polymeric Composites. *Journal of King Saud University - Engineering Sciences, in press*. doi: 10.1016/j.jksues.2017.01.005.

Agunsoye, J. O., Bello, S. A., **B**ello, L. and Idehenre, M. M. (2016a). Assessment of mechanical and wear properties of epoxy based hybrid composites. *Advances in Production Engineering & Management, 11*(**1**), 5-14. doi: 10.14743/apem2016.1.205.

Agunsoye, J. O., Bello, S. A., Talabi, S. I., Yekinni, A. A., A., R. I., D., O. A. and E., I. T. (2015). Recycled Aluminium Cans/Eggshell Composites: Evaluation of Mechanical and Wear Resistance Properties. *Tribology in Industry, 37*(**1**), 107-116.

Agunsoye, J. O., Bello, S. A., Yekinni, A. A., Raheem, I. A. and Awe, I. O. (2016b). *Aluminium alloy metal matrix composites: different eggshell particle sizes, a comparative study.* Paper presented at the UNILAG Annual Research Conference and Fair, Lagos *2-3*, 4-12.

Aigbodion, V. S. (2014). Thermal ageing on the microstructure and mechanical properties of Al–Cu–Mg alloy/bagasse ash particulate composites. *Journal of King Saud University - Engineering Sciences, 26*(**2**), 144-151. doi: http://dx.doi.org/10.1016/j.jksues.2013.01.003.

Akindapo, J. O., Harrison, A. and Monsur, S. (2014). Evaluation of Mechanical Properties of Coconut Shell Fibres as Reinforcement Material in Epoxy Matrix. *International Journal of Engineering Research & Technology (IJERT), 3*(**2**), 2337-2348.

Alaneme, K. K., Bodunrin, M. O. and Awe, A. A. (2016). Microstructure, mechanical and fracture properties of groundnut shell ash and silicon carbide dispersion strengthened aluminium matrix composites. *Journal of King Saud University - Engineering Sciences, in Press*. doi: 10.1016/j.jksues.2016.01.001.

Alaneme, K. K. and Sanusi, K. O. (2015). Microstructural characteristics, mechanical and wear behaviour of aluminium matrix hybrid composites reinforced with alumina, rice husk ash and graphite. *Engineering Science and Technology, an International Journal, 18*(**3**), 416-422. doi: 10.1016/j.jestch.2015.02.003.

America's Plastic Maker. (2016). Plastic Car and Bumper Systems. America: America's Plastic Maker 1-2.

Asuke, F., Abdulwahab, M., Aigbodion, V. S., Fayomi, O. S. I. and Aponbiede, O. (2014). Effect of Load on the Wear Behaviour of Polypropylene/Carbonized Bone Ash Particulate Composite. *Egyptian Journal of Basic and Applied Sciences, 1*(**1**), 67-70. doi: http://dx.doi.org/10.1016/j.ejbas.2014.02.002.

Asuke, F., Aigbodion, V. S., Abdulwahab, M., Fayomi, O. S. I., Popoola, A. P. I., Nwoyi, C. I. and Garba, B. (2012). Effects of bone particle on the properties and microstructure of polypropylene/bone ash particulate composites. *Results in Physics, 2*, 135-141. doi: http://dx.doi.org/10.1016/j.rinp.2012.09.001.

Atuanya, C. U., Edokpia, R. O. and Aigbodion, V. S. (2014). The physio-mechanical properties of recycled low density polyethylene (RLDPE)/bean pod ash particulate composites. *Results in Physics, 4*, 88-95. doi: http://dx.doi.org/10.1016/j.rinp.2014.05.003.

Atuanya, C. U., Ibhadode, A. O. A. and Dagwa, I. M. (2012). Effects of breadfruit seed hull ash on the microstructures and properties of Al–Si–Fe alloy/breadfruit seed hull ash particulate composites. *Results in Physics, 2*, 142-149. doi: http://dx.doi.org/10.1016/j.rinp.2012.09.003.

Bello, S. A. (2017). *Development and Characterisation of Epoxy-Aluminium-Coconut shell Particulate Hybrid Nanocomposites for Automobile Applications.* (Ph.D. Thesis), University of Lagos Lagos, Nigeria.

Bello, S. A., Agunsoye, J. O., Adebisi, J. A., Adeyemo, R. G. and Hassan, S. B. (2018a). Optimization of tensile properties of epoxy aluminum particulate composites using regression models. *Journal of King Saud University - Science, in press*. doi: https://doi.org/10.1016/j.jksus.2018.06.002.

Bello, S. A., Agunsoye, J. O., Adebisi, J. A. and Hassan, S. B. (2018b). Optimisation of charge ratios for ball milling synthesis: agglomeration and refinement of coconut shells. *Engineering and Applied Science Research (EASR), 42*(**4**), 262-272. doi: 10.14456/easr.2018.36.

Bello, S. A., Agunsoye, J. O., Adebisi, J. A., Kolawole, F. O. and Suleiman, B. H. (2106). Physical Properties of Coconut Shell Nanoparticles. *Kathmandu University Journal of Science, Engineering and Technology, 12*(**1**), 63-79.

Bello, S. A., Agunsoye, J. O., Adebisi, J. A. and Suleiman, B. H. (2017). Effects of Aluminium Particles on Mechanical and Morphological Properties of Epoxy Nanocomposites. *Acta Periodica Technological, 48*, 25-38.

Bello, S. A., Agunsoye, J. O. and Hassan, S. B. (2015a). Synthesis of Coconut Shell Nanoparticles Via A Top Down Approach: Assessment of Milling Duration on The Particle Sizes and Morphologies of Coconut Shell Nanoparticles. *Materials Letters, 159*, 514-519. doi: http://dx.doi.org/10.1016/j.matlet.2015.07.063.

Bello, S. A., Agunsoye, J. O., Hassan, S. B., Zebase Kana, M. G. and Raheem, I. A. (2015b). Epoxy Resin Based Composites, Mechanical and Tribological Properties: A Review. *Tribology in Industry, 37*(**4**), 500-524.

Bello, S. A., Hassan, S. B., Agunsoye, J. O. and Amuda, M., Olawale Hakeem. (2019). Nigeria Patent No. NG/P/2019/100. F. R. o. Nigeria

Bello, S. A., Hassan, S. B., Agunsoye, J. O., Kana, M. G. Z. and A, R. I. (2015c). Synthesis of Uncarbonised Coconut Shell Nanoparticles: Characterisation and Particle Size Determination *Tribology in Industry, 37*(**2**), 257-263.

Bello, S. A., Raheem, I. A. and Raji, N. K. (2015d). Study of tensile properties, fractography and morphology of aluminium (1xxx)/coconut shell micro particle composites. *Journal of King Saud University - Engineering Sciences*. doi: http://dx.doi.org/10.1016/j.jksues.2015.10.001.

Bhandakkar, A., Kumar, N., Prasad, R. C. and Sastry, S. M. L. (2014). Interlaminar Fracture Toughness of Epoxy Glass Fiber Fly Ash Laminate Composite. *Materials Sciences and Applications, 05*(**04**), 231-244. doi: 10.4236/msa.2014.54028.

Breitung-Faes, S. and Kwade, A. (2008). Nano particle production in high-power-density mills. *Chemical Engineering Research and Design, 86*(**4**), 390-394. doi: 10.1016/j.cherd.2007.11.006.

Davoodi, M. M., Sapuan, S. M., Ahmad, D., Ali, A., Khalina, A. and Jonoobi, M. (2010). Mechanical properties of hybrid kenaf/glass reinforced epoxy composite for passenger car bumper beam. *Materials & Design, 31*(**10**), 4927-4932. doi: 10.1016/j.matdes.2010.05.021.

Deng, C. F., Wang, D. Z., Zhang, X. X. and Li, A. B. (2007). Processing and properties of carbon nanotubes reinforced aluminum composites. *Materials Science and Engineering: A, 444*(**1-2**), 138-145. doi: 10.1016/j.msea.2006.08.057.

Deshpande, S. and Rangaswamy, T. (2014). Effect of Fillers on E-Glass/Jute Fiber Reinforced Epoxy Composites. *Int. Journal of Engineering Research and Applications, 4*(**8**), 118-123.

Essl, F., Bruhn, J., Janssen, R. and Claussen, N. (1999). Wet milling of Al-containing powder mixtures as precursor materials for reaction bonding of alumina (RBAO) and reaction sintering of aluminium-aluminide alloys (3A). *Materials Chemistry and Physics, 61*, 69-77.

Hassan, S. B., Agunsoye, J. O. and Bello, S. A. (2015). Characterization of Coconut Shell Nanoparticles using Electron Microscopes. *Proceedings of 10th UNILAG Annual Research Conference and Fair, 2-3*, 221-225.

Hassan, S. B. and Aigbodion, V. S. (2015). Effects of eggshell on the microstructures and properties of Al–Cu–Mg/eggshell particulate composites. *Journal of King Saud University - Engineering Sciences, 27*(**1**), 49-56. doi: http://dx.doi.org/10.1016/j.jksues.2013.03.001.

Hunton, P. (2005). Research on Eggshell Structure and Quality: An Historical Overview. *Brazilian Journal of Poultry Science, 7*(**2**), 67-71.

Janik, H., Sienkiewicz, M. and Kucinska-Lipka, J. (2014). Polyurethanes. 253-295. doi: 10.1016/b978-1-4557-3107-7.00009-9.

Kamberović, Ž., Romhanji, E., Filipović, M. and Korać, M. (2009). The Recycling of High Magnesium Aluminium Alloys Estimation of the Most Reliable Procedure. *MjoM, 15*(**3**), 189-200.

Knieke, C., Steinborn, C., Romeis, S., Peukert, W., Breitung-Faes, S. and Kwade, A. (2010). Nanoparticle Production with Stirred-Media Mills: Opportunities and Limits. *Chemical Engineering & Technology, 33***(9)**, 1401-1411. doi: 10.1002/ceat.201000105.

Liu, T., Shen, H., Wang, C. and Chou, W. (2013). Structure evolution of Y2O3 nanoparticle/Fe composite during mechanical milling and annealing. *Progress in Natural Science: Materials International, 23***(4)**, 434-439. doi: http://dx.doi.org/10.1016/j.pnsc.2013.06.009.

Manufacturer, N. C. o. I.-B. A. o. V. (2012). Automotive Industry and Sustainability. Brazil: National Confederation of Industries-Bazilian Association of Vehicle Manufacturer 1-45.

MatWeb Material Property Data. (2010). Azdel Plus C401-B01 40% Chopped Fiber Mat/PP Resin Matrix. 2010, from http://www.matweb.com/search/datasheet.aspx?MatGUID=c9cea89b3274415d89 2ea6af98f39647

Natarajan, K. and Balasubramanya, P. C. (2013). Mechanical and Morphological Study of Coir Fiber Reinforced International Journal of Emerging Technology and Advanced EngineeringModified Epoxy Matrix Composites. *International Journal of Emerging Technology and Advanced Engineering, 3***(12)**, 583-587.

Padmavathi, K. R. and Ramakrishnan, R. (2014). Tribological Behaviour of Aluminium Hybrid Metal Matrix Composite. *Procedia Engineering, 97*, 660-667. doi: 10.1016/j.proeng.2014.12.295.

Pargi, M. N. F., Teh, P. L., Hussiensyah, S., Yeoh, C. K. and Abd Ghani, S. (2015). Recycled-copper-filled epoxy composites: the effect of mixed particle size. *International Journal of Mechanical and Materials Engineering, 10***(1)**, 3. doi: 10.1186/s40712-015-0030-2.

Pokropivny, V., Lohmus, R., Hussainova, I., Pokropivny, A. and Vlassov, S. (2007). *Introduction to Nanomaterials and Nanotechnology*: Tartu University Press.

Prasad Yadav, T., Manohar Yadav, R. and Pratap Singh, D. (2012). Mechanical Milling: a Top Down Approach for the Synthesis of Nanomaterials and Nanocomposites. *Nanoscience and Nanotechnology, 2***(3)**, 22-48. doi: 10.5923/j.nn.20120203.01.

Rahman, M. H. and Rashed, H. M. M. A. (2014). Characterization of Silicon Carbide Reinforced Aluminum Matrix Composites. *Procedia Engineering, 90*, 103-109. doi: 10.1016/j.proeng.2014.11.821.

Sarki, J., Hassan, S. B., Aigbodion, V. S. and Oghenevweta, J. E. (2011). Potential of using coconut shell particle fillers in eco-composite materials. *Journal of Alloys and Compounds, 509***(5)**, 2381-2385. doi: http://dx.doi.org/10.1016/j.jallcom.2010.11.025.

Sommer, M., Stenger, F., Peukert, W. and Wagner, N. J. (2006). Agglomeration and breakage of nanoparticles in stirred media mills—a comparison of different methods and models. *Chemical Engineering Science, 61***(1)**, 135-148. doi: 10.1016/j.ces.2004.12.057.

The United Kingdom composites Industry. (2013). The United Kingdom composites industry – turning ideas into investments. *Reinforced Plastics, 57***(3)**, 43-46. doi: http://dx.doi.org/10.1016/S0034-3617(13)70095-X.

Wang, Z., Huang, X., Xian, G. and Li, H. (2016). Effects of surface treatment of carbon fiber: Tensile property, surface characteristics, and bonding to epoxy. *Polymer Composites, 37***(10)**, 2921-2932. doi: 10.1002/pc.23489.

Wang, Z. L. (2000). Transmission Electron Microscopy of Shape-Controlled Nanocrystals and Their Assemblies. *J. Phys. Chem. B, 104*, 1153-1175.

Wang, Z. L. (2003). New Development in Transmission Electron Microscopy for Nanotechnology. *Advanced Materials, 15***(18)**, 1498-1514. doi: 10.1002/adma.200300384.

Zhang, X., Fan, X., Yan, C., Li, H., Zhu, Y., Li, X. and Yu, L. (2012). Interfacial microstructure and properties of carbon fiber composites modified with graphene oxide. *ACS Appl Mater Interfaces, 4***(3)**, 1543-1552. doi: 10.1021/am201757v.